A Multitechnique Characterization of Dealuminated Mordenites

B. L. MEYERS, T. H. FLEISCH, G. J. RAY, J. T. MILLER, AND J. B. HALL

Amoco Research Center, P.O. Box 400, Naperville, Illinois 60566

Mordenite zeolites were altered both physically and catalytically by dry thermal treatments, acid leaching at mild temperatures, sequential thermal/acid treatments, and hydrothermal steaming. Good agreement was demonstrated between four diverse analytical procedures, X-ray diffraction (XRD), X-ray photoelectron spectroscopy (XPS), ^{29}Si and ^{27}Al nuclear magnetic resonance (NMR), and NH$_3$ temperature-programmed desorption (TPD) and the extent of dealumination. The complementary nature of ^{29}Si and ^{27}Al NMR in characterizing the Al content over broad concentrations was demonstrated. Both XRD and NMR showed that dry heat treatments alone expelled as much as 70% of the aluminum from the framework of the fresh mordenite, but XPS showed no change in the surface aluminum concentration. Strong zeolite acidity as measured by TPD of NH$_3$ above 290°C was nearly completely destroyed or made inaccessible by dry thermal treatment. This acidity was restored by acid leaching which removed the detrital aluminum, making the remaining tetrahedral aluminum sites accessible to NH$_3$. Acidity decreases *faster* than residual structural aluminum content, possibly because a progressively larger fraction of the structural aluminum is in partially inaccessible four-member rings. Unlike the results obtained with NH$_3$, fresh mordenites had very little strong acidity when measured by a larger molecule such as *t*-butylamine. But dealumination by HCl increased the accessibility of such acid sites to these larger molecules. The thermally dealuminated mordenite was hydrothermally dealuminated and analyzed by ^{27}Al NMR and XPS. Roughly 40% of the remaining tetrahedral aluminum is lost from the structure upon steaming at 500°C for 70 h. Here, XPS detects modest increases in surface aluminum concentration which were not observed for the heat-treated samples. This shows that steam is required for expelled aluminum to migrate to the zeolite surface. Acid dealumination of these mordenites was shown by N$_2$ adsorption to develop maximum micropore volume and to minimize external zeolite surface area. The changes observed do not fully explain the aging characteristics during methanol conversion exhibited by deeply dealuminated mordenites; however, changes in catalyst selectivity toward higher-molecular-weight products can be explained by increases in the micropore volume following acid dealumination. © 1988 Academic Press, Inc.

INTRODUCTION

The synthesis of high silica zeolites, especially sieves of the pentasil family, has sparked interest in reformulating older, high-alumina zeolites, such as faujasites and mordenites, into highly siliceous compositions. Mordenites, for instance, have been dealuminated by reaction with acids (*1*), with SiCl$_4$ vapors (*2*), by steaming and acid treatments (*3*), and by cyclic steaming and acid leaching treatments (*4*). An excellent review on the preparation and characterization of aluminum-deficient zeolites has recently been published (*5*).

Dealumination of mordenites has been reported to produce large and frequently favorable changes in catalytic performance. Topohieva *et al.* (*6*) reported an increase in cumene cracking activity of acid dealuminated mordenites. Weller and Brauer (*7*) found that hexane cracking activity increased as mordenites were dealuminated. Sand and co-workers (*8*) studied mordenites with Si/Al ratios ranging over two orders of magnitude and found complex changes in cracking, hydrocracking, and isomerization properties as a function of aluminum content. The increase in adsorptive capacity and diffusion rates, especially in the one-dimensional mordenite structure, appear to more than compensate for the loss in the number of catalytic sites as dealumination progresses. Optimum se-
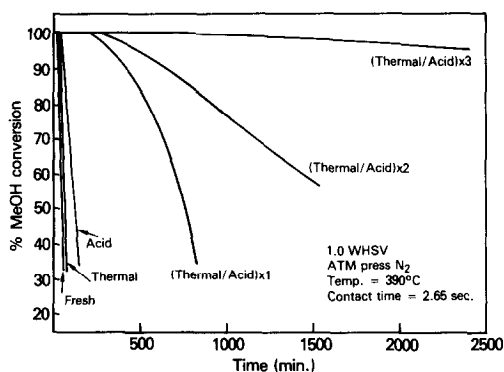
FIG. 1. Methanol conversion vs time over dealuminated mordenites.

lectivity for each reaction is a compromise of these and other opposing factors.

Mordenites have been investigated for the conversion of methanol to gasoline, a reaction that in previous studies showed rapid deactivation (9–12). In our own study with dealuminated mordenites, it was found that the life of the gasoline conversion reaction increased as the aluminum content of the zeolite decreased (Fig. 1). Highly dealuminated mordenites exhibited activity for over 100 h when the structural aluminum concentration was reduced to less than about 0.7%. The dramatic change in the deactivation characteristics for this large-pore zeolite after dealumination leads us to more thoroughly investigate its chemical and physical structure as a function of aluminum content.

An understanding of the factors which lead to rapid coking and deactivation is essential for development of optimum catalysts. Since mordenites can easily be dealuminated over wide ranges and aluminum plays an important role in coking, this study is a logical extension of our previous work on dealuminated faujasites (13, 14). In addition modified mordenites might find more widespread use in petroleum and chemical refinery processes because they are hydrothermally more stable than faujasites. However, to become more useful the problem of rapid activity loss due to coking

and plugging of the two-dimensional pore structure must be minimized.

EXPERIMENTAL

A. Catalyst Preparation

A commercially available H-mordenite, obtained from Norton Chemical Co., was used as the starting material. The H-mordenite was subjected to one of several dry thermal, acid, or thermal plus acid treatments to affect dealumination. The catalysts and treatments are listed in Table 1. The aluminum content was determined by bulk chemical analysis, and the crystallinity was determined by XRD using the commercial H-mordenite as a 100% crystalline reference. Sodium content was less than 500 ppm in all starting mordenites.

Thermal treatment. H-mordenite samples were initially dried at 110°C under vacuum for 2 to 4 h. Approximately 25 g of dried, finely powdered sample was heated in a muffle furnace at a temperature of 750°C in air for 8 h.

Acid treatment. Twenty-five grams of H-mordenite was slurried in 400 ml of 5 M HCl. The samples were heated under reflux for 4 h, cooled, and filtered. The catalysts were washed twice by stirring in 250 ml of H_2O for 15 min and refiltering. The wet samples were dried overnight at 110°C under vacuum and for an additional hour at 400°C.

TABLE 1

Fresh Mordenite and Dealumination Procedures Studied

Sample	Treatment	Al content (wt%)
Fresh	None	6.03
Heat	750°C, 8 h	6.03
Acid	5 M HCl, 4-h reflux	2.19
(Heat/acid) 1X	700°C/5 M HCl reflux	1.11
(Heat/acid) 2X	700°C/5 M HCl reflux	
	725°C/5 M HCl reflux	0.71
(Heat/acid) 3X	700°C/5 M HCl reflux	
	725°C/5 M HCl reflux	
	750°C/5 M HCl reflux	0.75

Thermal/acid treatment. One hundred grams of fresh, dry H-mordenite was heated at 700°C for 8 h in air. Following the thermal treatment, the zeolite was refluxed in 400 ml of 5 M HCl for 4 h. The zeolite was filtered and washed with 250 ml water. The wet sample was dried overnight at 110°C under vacuum and heated at 400°C for an additional hour.

A portion of the thermal/acid dealuminated mordenite was subjected to further thermal/acid treatments. On the second and third treatments the calcination temperature was increased to 725 and 750°C, respectively.

B. Catalytic Measurements

The conversion of methanol was carried out using 4.5 g (7.3 cc) of catalyst placed in a fixed-bed, continuous flow reactor under atmospheric nitrogen. The catalyst powder was mixed with water and pressed into 3-cm-diameter × 1-cm-cylindrical pellets. The pellets were dried at 200°C and crushed. The particles were screened to pass 12 mesh (U.S. Standard) and retained on a 20-mesh screen. The reactor was a 1.4-cm-i.d. × 45-cm-tubular quartz reactor with an internal thermowell. The nitrogen carrier gas was 165 cc/min (contact time, 2.65 s). The methanol feed rate was 4.5 g/h (WHSV, 1.0 g/methanol/h/g catalyst). The reaction temperature was 390°C. The reaction products were analyzed by off-line gas chromatography ($\frac{1}{8}$ in. × 6 ft, *n*-octane on porasil C). The deactivation of the catalysts was monitored by analyzing the products every 30 to 60 min. The conversion was defined by the fraction of methanol (or dimethyl ether) reacted to hydrocarbons.

C. Analytical Methods

XRD. Two grams of sieve were intimately mixed with 10–15% NBS, silicon powder (used as an internal standard), and the materials were equilibrated with laboratory air overnight. Samples were studied on the Scintag PAD-V diffractometer. Copper radiation was employed with an energy dis-

persive detector. Tube voltage was 40 kV and tube current 30 mA. The sample was continuously scanned from 42 to 62°, 20 with a scan rate of 0.1°/min. Unit cell dimensions were determined employing a program with the following reflections: (0,10,0), (6,8,0), (0,0,4), (10,0,0), (7,1,3), (5,3,4), (8,4,3), and (8,8,2).

TPD. Temperature-programmed desorption (TPD) of *t*-butylamine to determine catalyst acidity has previously been reported (*15*). The high-temperature peak (200–300°C) historically has been taken as an indication of the amount of strong acid sites. Alternatively, NH_3 was the probe molecule and again the highest temperature peak was taken as a measure of strong acidity. Recently both procedures have been refined by trapping the evolved gases in an aqueous solution buffered at pH 5 and which was continuously titrated with 0.01 N HCl to maintain this pH as desorbed NH_3 or amines were evolved. The automatic titrator employed was a Metrohm/655 Dosimat. This refinement of the procedure rules out the variable responses which could be produced in thermal conductivity measurements by varied amine cracking patterns.

Surface area and micropore volumes. Samples were analyzed on the Micromeritics Corp. Digisorb Model 2500. Total surface area, mesoporosity, and its associated surface area, as well as micropore volumes derived from *t* plots were all calculated by conventional procedures (*16–18*). "External surface area" was arbitrarily defined as the difference between total surface area via the BET method and the calculated mesopore surface area.

NMR. Both ^{27}Al and ^{29}Si NMR spectra were obtained on a Nicolet NT-300 spectrometer operating at 7.05 T and equipped with a broadband Chemagnetics MAS probe. ^{29}Si spectra were obtained using a spectral width of 10 kHz. Data were acquired in 512 data points which were zero-filled to 2K after using a Gaussian line broadening of 100 Hz. An 8.5-μm (45°) excitation pulse, 2.0-s relaxation delay, and

2000 acquisitions were used. ^{29}Si chemical shifts were referenced to tetramethylsilane (TMS) by using an external sample of hexamethyldisiloxane which has a chemical shift of 6.7 ppm from TMS. ^{27}Al spectra were obtained using a spectral width of 30 to 80 kHz. Data were acquired in 256 data points which were zero-filled to 2K after using a trapezoidal multiplication on the last 30 data points of the FID. A 2.5-μs (16°) excitation pulse, 0.1-s relaxation delay, and 4000 acquisitions were used. The ^{27}Al chemical shifts were referenced to a solution of aqueous AlCl$_3$. Bullet rotors with an internal diameter of 7 mm and a height of 12 mm were used and spinning rates were between 3 and 5 kHz.

XPS. The sample surfaces were analyzed in a Hewlett–Packard 5950B electron spectrometer. The sample powders were pressed into 6-mm-diameter pellets with a thickness of approximately 1 mm, which, in turn, were put into sample holders. Monochromatic Al$K\alpha$ ($h\nu$ = 1486.6 eV) radiation was used providing linewidths on the order of 0.80 eV FWHM for the Au $4f_{7/2}$ photoelectron line. A 2 × 8-mm section of the sample surface was analyzed. Sample charging was minimized by the use of an HP electron flood gun which produces low-energy electrons (<5 eV) to the sample surface during XPS analysis. Elemental concentrations were calculated after correcting Si $2p$, Al $2p$, O $1s$, and C $1s$ peak areas for instrumental parameters, differences in photoionization cross section, and differences in electron mean free path.

RESULTS AND DISCUSSION

Table 1 lists the samples used in this study. Throughout the manuscript we will use the following abbreviations: fresh (untreated commercial H-mordenite), heat (1400°F, 8 h in air), acid (refluxed in 5 M HCl for 4 h), and heat/acid (combinations of heating followed by acid washing).

TPD

Catalyst acidity and effective diffusivity of larger hydrocarbon-type molecules appear to be two of the most important properties which can affect catalytic performance of zeolites. A measure of both these properties is gained from a TPD study of fresh and acid extracted mordenites using a small, strongly basic probe molecule such as NH$_3$ and a much larger, basic molecule such as *t*-butylamine. Figure 2 shows typical TPD spectra of NH$_3$ for a fresh sample, a heated sample, an acid washed sample, and a two-cycle calcined/acid refluxed sample. Figure 3 shows the evolution of *t*-butylamine from the same mordenites, and Table 2 summarizes all TPD data.

High-surface-area, microporous solids readily physisorb ammonia at room temperature. To minimize the physical adsorption, exposure of NH$_3$ was done at an elevated temperature (70°C), followed by a helium purge for 1 h at 70°. Even with these precautions, some weakly bound NH$_3$ is always measured. Under the experimental conditions, the amount of total NH$_3$ desorbed increased approximately with increasing structural aluminum content of the mordenite.

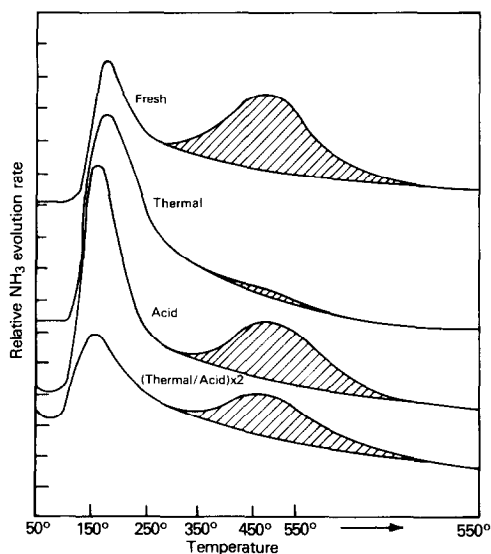Strongly bound NH$_3$ desorbed from the fresh mordenite is depicted by the shaded

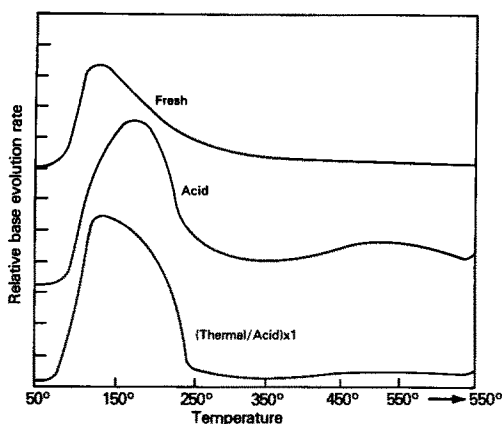FIG. 2. TPD of NH$_3$ from dealuminated mordenites.

FIG. 3. TPD of *t*-butylamine from selected mordenites.

portion in Fig. 2 and tabulated in Table 2. High-temperature NH_3 desorption starts at 290°C, peaks at 475°C, and continues for at least 30 min at the maximum temperature reached, namely 550°C. This peak was integrated as shown in Fig. 2. This interaction assumes that there is a tailing of the low-temperature peak and uses this "tail" as the "baseline" for the high-temperature desorption. Results are consistent with a progressive dealumination but could be biased low for the high-temperature peak. The amount of NH_3 desorbed at high temperatures was taken as a measure of strong acidity. Using this definition, 45% of the fresh mordenite aluminum can be considered strongly acidic. The heat dealuminated mordenite has almost no strong acidity. In the acid leached mordenite, 35% of the aluminum is strongly acidic. On further dealumination, e.g., in the heat/acid series, the relative percentage of strongly acidic aluminum continues to drop, finally reaching 15% in the 3X sample.

In mordenite, there are four crystallographic sites in a ratio of $1:1:2:2$. Assuming a random distribution of aluminum, one-third of the aluminum would be in four-membered rings. One-half of these would face a twelve-ring channel and be accessible to ammonia while the other half would

face an eight-ring channel and would be difficult to access by ammonia, especially if the channel is obstructed. Therefore, in a fresh mordenite with a total of 6.0% aluminum, approximately 1.0% aluminum could be inaccessible to NH_3. This percentage could be higher if the aluminum is nonrandom and is preferentially located in the four-membered rings (19, 20). As dealumination proceeds and accessible aluminum is removed, a larger fraction of the framework aluminum remains in positions partially inaccessible to NH_3. Alternatively, some amorphous alumina may be occluded in small eight-ring pores which may not be removed by acid extraction. Therefore, elemental analysis detects the presence of aluminum that does not give rise to measurable acidity.

The heat-treated sample was estimated by NMR to have lost approximately 70% of the original aluminum from the framework, and this amorphous aluminum is nonacidic or weakly acidic. The lack of strong acidity compared with the acid dealuminated mordenite of comparable tetrahedral aluminum content indicates that the amorphous aluminum from thermal dealumination remains in the zeolite pores blocking access to all but a trace of the strongly acidic aluminum remaining in the zeolite lattice. Strong acidity is again observed on thermally dealuminated mordenites subsequently subjected to acid extraction, i.e.,

TABLE 2

Acidity of Aluminium-Deficient Mordenites as Measured by TPD of NH_3 and TBA[a]

	Absolute Al	Total NH_3	High temp. NH_3	High temp. NH_3/Al[b]	High temp. TBA	High temp. TBA/Al[b]
Fresh	2.20	1.70	0.72	45	~0	0
Heat	2.20	0.92	Trace	~0	N.D.	N.D.
Acid	0.81	1.07	0.28	35	0.14	17
(Heat/acid) 1X	0.41	0.53	0.11	27	0.036	9
(Heat/acid) 2X	0.26	0.31	0.04	15	~0	~0
(Heat/acid) 3X	0.27	0.19	0.04	15	N.D.	N.D.

[a] All units are m-moles/g unless otherwise stated.
[b] Relative percentage base compared to Al present in this sample.

(heat/acid) 1X mordenite. The acid treatment dissolves the amorphous aluminum exposing the remaining structural aluminum to NH_3.

Strong acidity measured by TPD of t-butylamine (TBA) reveals a different pattern from that of NH_3 desorption. Whereas 45% of the aluminum sites strongly adsorbed NH_3 in the fresh mordenite, it does not exhibit any high-temperature TBA desorption. Despite the lower aluminum content and the reduction in the number of acid sites, more TBA is strongly adsorbed on the acid dealuminated mordenite than that on fresh mordenite. Acid extraction increased the accessibility of strong acid sites to the larger TBA molecule because the 5 M HCl dissolves nonframework silica–alumina from the fresh zeolite pores. For the acid dealuminated mordenite, TBA measures approximately 50% as much strong acidity as NH_3. Few strong acid sites are measured by TBA for highly dealuminated mordenites.

NMR

The loss of aluminum from the mordenite lattice is confirmed by ^{29}Si and ^{27}Al NMR. The ^{29}Si NMR spectra of the mordenite samples are shown in Fig. 4. Four broad peaks are observed at −95, −100, −106, and −112 ppm, and these are assigned to Si(nAl) where n = 3, 2, 1, and 0, respectively. The intensities of all the peaks are reduced following dealumination by heat, acid, or heat plus acid treatment except for the −112 ppm peak, which becomes more intense. For highly dealuminated samples, the latter peak is resolved into three peaks at −112.8, −113.8, and −115.6 ppm with relative intensities of 2 : 1 : 3. Other workers have observed similar results for mordenite and its dealuminated products (21–23). The unit cell of mordenite is known to have four crystallographically distinct silicons in the ratio 1 : 1 : 2 : 2, but only three of the four nonequivalent silicon lattice positions are resolved by ^{29}Si NMR, accounting for the 2 : 1 : 3 ratio of intensities. The Si/Al ratio of
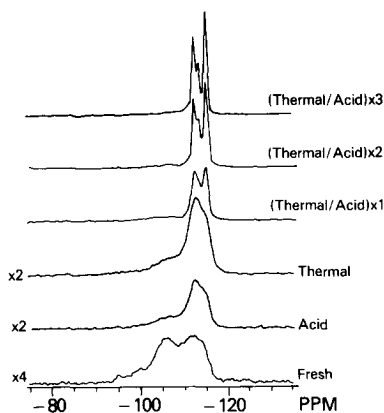

FIG. 4. ^{29}Si NMR spectra of treated mordenites.

the lattice framework was calculated from the ^{29}Si NMR data using the following equation (24, 25),

$$Si/Al = \sum_{n=0}^{4} I_{Si(nAl)} \Big/ \sum_{n=0}^{4} 0.25\, n\, I_{Si(nAl)},$$

where $I_{Si(nAl)}$ is the intensity of the peak attributable to Si(nAl) units. The Si/Al ratio for each sample is given in Table 3. For the most highly dealuminated mordenites, e.g., (heat/acid) 3X, there was only a weak Si(1Al) peak, and therefore, their Si/Al ratio could only be estimated.

From the Si/Al ratio determined by ^{29}Si NMR, the *relative* tetrahedral aluminum content for each sample was calculated and compared to the relative aluminum content by elemental analysis as shown in Table 3 and plotted in Fig. 8. Except for the heat dealuminated mordenite (see below), the agreement is quite good.

Above a Si/Al ratio of about 50, ^{29}Si NMR can only be considered qualitative because a precise determination of the Si/Al ratio is not possible due to the low peak intensities of the Si(1Al) peak. However, an increase in the resolution of the Si(0Al) peak provides evidence that dealumination has continued.

The intensity of the ^{27}Al signal is a sensitive function of quadrupole coupling of the aluminum nucleus (26, 27). Consequently,

TABLE 3

Silicon/Aluminum Ratios via ^{29}Si and ^{27}Al NMR vs Relative Aluminum Contents

Sample	Si NMR		Relative Al by elemental analysis	Al NMR	
	Si/Al	Relative Al (tetrahedral)		Total (intensity)	55 ppm peak only[b]
Fresh	5.5	100	100	100	100
Heat	18	34	100	34[a]	18
Acid	15	41	36	30	23
(Heat/acid) 1X	27	23	18	13	9.2
(Heat/acid) 2X	~50	12	12	10	6.5
(Heat/acid) 3X	~50	12	12	7	4.4

[a] Maximum value which is biased low because of amorphous Al present which contributes weakly to total signal.

[b] Intensities are expressed relative to the 55 ppm peak of the fresh sample set equal to 100%. This process ignores the intensity of the sidebands.

^{27}Al NMR is a less reliable technique than ^{29}Si NMR for determining the relative concentrations of aluminum in different environments within a given sample. However, for aluminum in the tetrahedral environment of the mordenite crystal lattice, relative aluminum concentrations for the dealuminated mordenites can be determined quantitatively by ^{27}Al NMR with a lower limit of detectability on the order of 100 ppm.

The ^{27}Al spectra are shown in Fig. 5. An intense peak at 55 ppm is assigned to aluminum in tetrahedral sites while weak peaks at 95 and 15 ppm are due to spinning sidebands resulting from magic-angle spinning. Additionally, the heat and acid dealuminated mordenites have a weak peak near 0 ppm that is assigned to aluminum (3+) ion in an octahedral coordination. A broad peak underlies the entire spectrum of the heat dealuminated mordenite. This peak is only detected with this sample and is assigned to amorphous aluminum oxide/hydroxide species. Except for the heat dealuminated mordenite, nearly all of the intensity of the ^{27}Al NMR spectra is due to tetrahedral aluminum with octahedral aluminum being present at only a few percent.

Comparisons of the total amount of alu-

minum present in the samples, relative to the fresh mordenite, were made by both elemental analysis and ^{27}Al NMR, and these data are also given in Table 3. There is good agreement between elemental analysis and the total ^{27}Al NMR intensities for all samples except the heat dealuminated mordenite.

The amorphous aluminum oxides detected in the heat dealuminated mordenites are formed from the aluminum that has left the lattice, and which, in the absence of an acid wash, remains in the sample. The amorphous aluminum has low symmetry, which results in a larger quadrupolar inter-
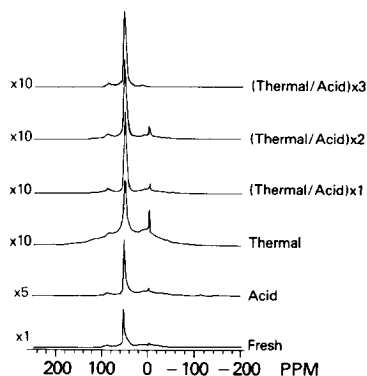

FIG. 5. ^{27}Al NMR spectra of treated mordenites.

(0 hour)

(0.5 hours)

(1.0 hour)

(5 hours)

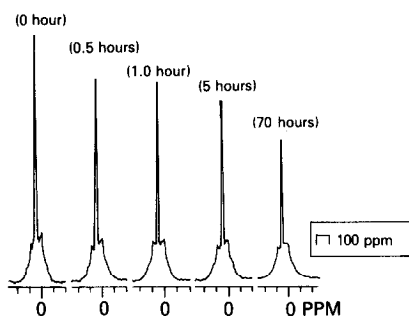(70 hours)

□ 100 ppm

0   0   0   0   0 PPM

FIG. 6. ^{27}Al NMR spectra of steamed mordenites. The starting sample was the heat dealuminated mordenite.

action than is experienced by the more symmetric tetrahedral aluminum in the lattice. The intensty of the NMR signal from a given number of aluminum nuclei experiencing a large quadrupolar coupling will be only a fraction of that given by an equal number of aluminum nuclei experiencing a smaller quadrupolar coupling (26, 27). As a result, the total NMR aluminum intensity for the heat dealuminated mordenite is less than that observed for fresh mordenite, even though both samples have the same amount of aluminum by elemental analysis.

The extent of dealumination of a given sample can be followed by measuring only the intensity of the tetrahedral aluminum peak at 55 ppm. The percentage of tetrahedral aluminum based on the 55 ppm peak intensities is given in Table 3 and is found to decrease as elemental aluminum decreases showing progressive dealumination. With aluminum NMR, dealumination can be followed to lower aluminum levels and complements the results obtained by ^{29}Si NMR.

The thermally dealuminated mordenite was subjected to steaming for 0.5 to 70 h at 500°C. The ^{27}Al NMR spectra of these samples are shown in Fig. 6 as a function of steaming time. The two prominent features of the spectra are the broad peak due to amorphous aluminum and the sharp peak due to aluminum in tetrahedral lattice position. Table 4 gives the total aluminum intensity of each steamed sample and the intensity of the tetrahedral aluminum as measured by the peak at 55 ppm. The progressive decrease in both of these measured intensities with steaming time is attributable to the further loss of tetrahedral framework aluminum. Steaming at 500°C for 70 h has resulted in the further loss of between 30% (from total NMR intensity) and 40% (from tetrahedral intensity) structural aluminum of the heat dealuminated mordenite.

XRD

XRD unit cell parameters of these mordenites are summarized in Table 5. All three unit cell dimensions are reduced by heat dealumination at 750°C, showing that significant amounts of aluminum can be expelled from the crystal lattice by dry heat treatment. The acid dealuminated mordenite also shows contractions in all three lattice dimensions. Although a_0 continues a very slow contraction with progressive dealumination, there is no further contraction of b_0 and c_0. To the contrary, b_0 and c_0 start a gradual expansion. The net result is a small increase in unit cell volume as the aluminum level approached the lowest level of 0.75%. For these samples, the dimension of a_0 was found to fit the following empirical equation,

TABLE 4

Aluminum Content of Steamed Mordenites via ^{27}Al NMR

Sample	Hours steaming	Percentage Al[a]	
		%TOT	55 ppm peak only
Heated	0.0	100.0	50.2
Steamed	0.5	86.4	40.2
Steamed	1.0	85.5	37.7
Steamed	5.0	80.7	34.7
Steamed	70.0	71.6	29.8

[a] %TOT is the total Al intensity measuring relative to the heated sample which was set at 100%. The intensities at the 55 ppm peak are also relative to *total* intensity of heated sample.

TABLE 5

Unit Cell Dimensions of Aluminum-
Deficient Mordenites

Sample and treatment	Å			Volume (Å^3)
	a_0	b_0	c_0	
Fresh	18.166	20.326	7.496	2767.8
Heat	18.092	20.292	7.465	2740.5
Acid	18.083	20.242	7.455	2728.9
(Heat/acid) 1X	18.069	20.261	7.463	2731.3
(Heat/acid) 2X	18.066	20.273	7.462	2733.0
(Heat/acid) 3X	18.063	20.285	7.464	2734.8

$$a_0 = 18.059 + (0.0085)(\%Al)$$
$$+ (0.0015)(\%Al)^2,$$

where (%Al) is the structural aluminum. Using the measured a_0 unit cell dimension and the above equation, the structural aluminum percentage can be determined. Others have also observed that the cell dimension changes in a complex way with dealumination (28).

XPS

The XPS data indicate that for all samples the Si/Al ratio at the crystallite surfaces is nearly identical to that of the bulk sample (see Table 6). For the heat dealuminated mordenite, XRD and NMR clearly show a loss of approximately 70% structural aluminum. However by XPS, there was no change in the concentration of surface aluminum during thermal dealumination, an indication that the nonstructural aluminum remains within the pore channels. This observation is also supported by the lower micropore volume of this sample. Thermal treatment followed by acid extraction reduces the surface aluminum concentration. The surface Si/Al ratio of the thermal/acid sample is nearly identical to the bulk Si/Al ratio. Acid treatment effectively removes all of the nonstructural aluminum, both within the pore and at the crystallite surface. This is confirmed by the disappearance of the broad amorphous aluminum band in the ^{27}Al NMR and the in-

crease in the micropore volume. The removal of the nonstructural aluminum from the zeolite pores by acid extraction also restores acidity to the mordenite. In recent work on steam dealumination of faujasite it was observed that the aluminum ions migrate to the crystallite surface during dealumination (9, 10). The aluminum surface concentration was found to increase logarithmically with treatment times. The observation here is that there is no aluminum ion migration to the mordenite surface during dry, thermal dealumination. This suggests that the migration of the expelled aluminum requires steam.

The heat-treated mordenite, which contains approximately 70% nonstructural and 30% structural aluminum, was further treated with 1 atm of steam at 250 and 500°C to determine if the nonstructural aluminum (present at a concentration of about 4%) could be induced to migrate to the crystallite surfaces. Steaming at 500°C did result in aluminum ion migration as shown by the increasing Al/Si atomic ratios (Fig. 7). The Al/Si ratio increases logarithmically with steaming time from about 0.14 after 1 h to about 0.18 after 70 h. However, this increase is rather small compared with earlier work on faujasite steam dealumination (13, 14). Comparable steaming of a US–Y zeolite at 500°C resulted in the expulsion and migration to the crystallite surface of about 4% aluminum resulting in an increase in the Al/Si surface atomic ratio from about 0.5 to 1.0.

TABLE 6

XPS Data on Treated Mordenites

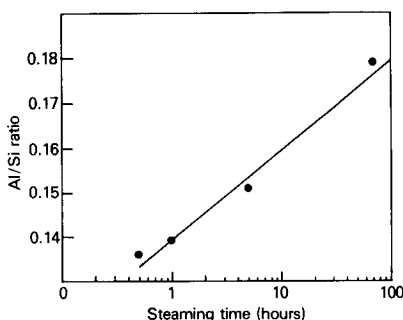| Sample	% Al[a]	Si/Al
Fresh	3.60	7.2
Heat	3.70	7.2
Acid	0.90	30
(Heat/acid) 1X	0.90	33
(Heat/acid) 2X	0.45	69
(Heat/acid) 3X	0.35	91

[a] Atomic percent (surface).

FIG. 7. Al/Si ratio by XPS of heat dealuminated mordenite steamed at 500°C.

Comparison of mordenite and faujasite indicates that the thermally expelled aluminum has little or no mobility during the subsequent steaming. The steaming leads to further structural aluminum loss as evidenced by [17]Al NMR, Table 4, and provides sufficient new nonstructural aluminum (about 0.5%) to account for the observed aluminum surface enrichment. It is possible that the amorphous aluminum expelled during dry heating polymerizes to a relatively high-molecular-weight, mixed oxide/hydroxide structure which cannot be mobilized upon subsequent steaming. Steaming at 250°C is a lower limit for dealumination and aluminum migration as the increase in Al/Si surface ratios at 250°C is barely above experimental error.

TEM

TEM micrographs of the fresh mordenite reveal two phases (see Fig. 8). The major phase (possibly as large as 90%) is the relatively dense material shown in the micrograph. This phase was determined by selected area electron diffraction (SAED) to be crystalline. The minor phase (greatly exaggerated in this single micrograph) is a porous phase, which was determined to be amorphous. It is well known how difficult it is to determine a minor amorphous phase in a crystalline material by XRD so microscopy of crystalline catalysts is advised to look for minor amorphous phases. This mi-

nor porous phase is likely a primary source of the measured "external surface area" of the fresh mordenite. Both phases were shown to have the same elemental composition using energy dispersive X-ray analysis.

TEM micrographs of the acid-treated mordenite show only the denser, crystalline phase, except now there is evidence of mesopore formation by the acid treatment (Fig. 9). This micrograph reveals numerous circular pores which range in diameter from about 50 to 500Å.

Surface Area, Mesoporosity, and Micropore Volume

Mordenite morphology changes upon heat, acid, and sequential heat/acid dealumination. Indications of structural changes are evidenced from the surface area and porosity data shown in Table 7. The fresh mordenite has relatively low total surface area and low internal zeolite microporosity. It does exhibit considerable "external surface area" probably due to the amorphous silica–alumina which is present from the original synthesis. The lack of acidity on the fresh mordenite as measured by TBA suggests that this silica–alumina is not strongly acidic. From the low micropore volume of fresh samples it appears that there is considerable amorphous material blocking or filling the micropores. The effect of this amorphous material is reflected in the hydrocarbon selectivity for methanol conversion, Table 8. The fresh and heat dealuminated mordenite have a high propane/propylene selectivity and low butane/pentane selectivity when compared to the acid-treated sieves. In addition, over the fresh and heat dealuminated mordenite the isobutane to normal butane ratio is abnormally low. The low yields of C_4 and C_5 products and the low iso/normal butane ratio suggests that there is amorphous material in the pore channels which sterically restricts the formation of the more bulky products, e.g., isobutane. Once the noncrystalline material is removed by acid ex-

MEYERS ET AL.

FIG. 8. Thin section TEM of fresh mordenite.

traction, however, isobutane and C_{4+} hy-
drocarbons are more readily formed.
   Heat dealumination at 750°C increased

micropore volume and surface area to val-
ues intermediate between those obtained
for fresh and acid-treated mordenites. Re-

TABLE 7

Surface Area, Mesoporosity, and Micropore Volume of
Aluminum-Deficient Mordenites

Sample	Total surface area[a] (m^2/g)	External & mesopore surface area[d] (m^2/g)	Mesopore volume[b] (cc/g)	Average mesopore radius[b] (Å)	Micropore volume[c] (cc/g)
Fresh	233	104	0.113	21	0.067
Heat	321	56	0.079	52	0.114
Acid	433	41	0.169	132	0.169
(Heat/acid) 1X	444	80	0.106	33	0.159
(Heat/acid) 2X	456	99	0.141	38	0.165
(Heat/acid) 3X	428	90	0.155	47	0.162

[a] BET method (16).
[b] Reference (17).
[c] From t plots.
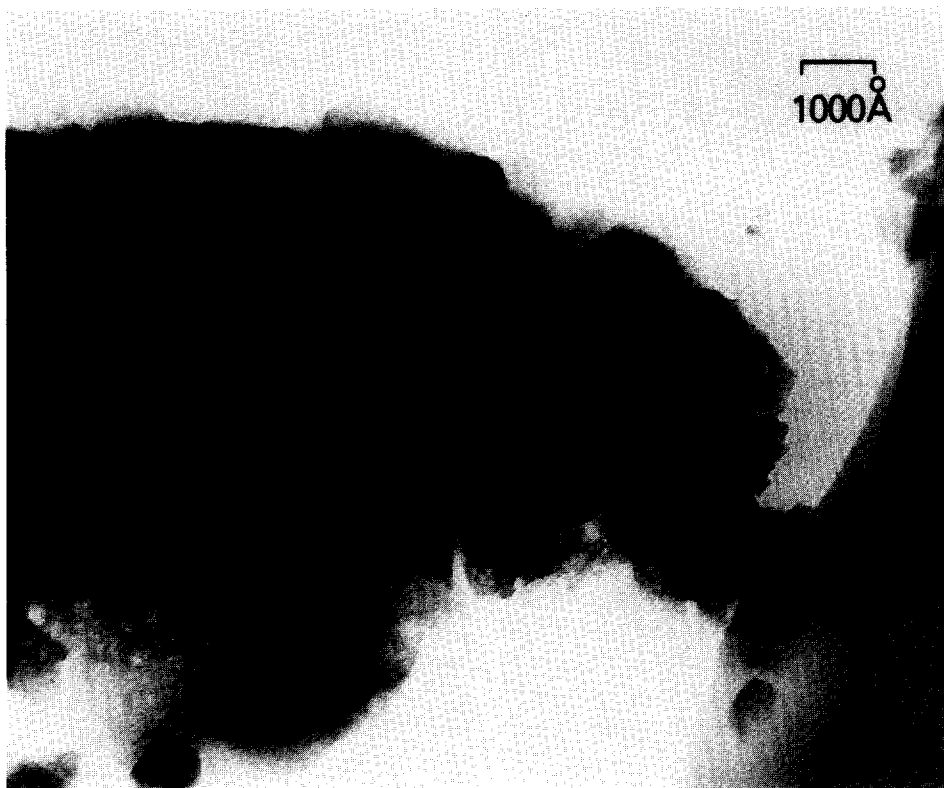[d] Via difference (see text).

FIG. 9. Thin section TEM of acid-treated mordenite.

fluxing with 5 M HCl increases the micropore volume to its maximum value and also increases total surface area, but decreases external surface area. The acid washed sample would appear to give the best combination of high microporosity, high internal surface area, and low external area. The external pores are large in diameter and contribute little to external area. Despite these morphological properties, this catalyst has only a slightly longer life than that of the fresh mordenite. As noted earlier,

TABLE 8

Hydrocarbon Distribution for Methanol Conversion over Mordenite[a]

Catalyst	Fresh	Heat	Acid	Thermal/acid		
				1X	2X	3X
Hydrocarbon products (wt%)						
CH_4	14.4	6.0	6.4	6.5	3.5	1.9
Tot C_2	17.2	23.6	18.1	11.4	4.9	3.5
Tot C_3	49.8	43.0	25.8	27.0	36.5	38.6
Tot C_4	11.1	13.1	27.9	33.4	32.3	33.3
Tot C_{5+}	5.8	11.9	21.8	22.8	22.8	22.7
i/n C_4H_{10}	1.36	0.85	5.48	9.05	10.1	11.9

[a] $T = 390°C$; N_2 flow = 165 cc/min; contact time = 2.65 s; WHSV = 1.0 h-liter.

TABLE 9

Relative and Absolute Al Content via Various Analytical Procedures

Sample	Absolute Al	Relative Al	Relative change in XRD, a_0	Relative Al via ^{29}Si NMR	Relative Al via ^{27}Al NMR	TPD[a] of NH$_3$	XPS
Fresh	6.03	100	100	100	100	100	100
Heat	6.03	100	37	41	34[b]	0	103
Acid	2.19	36	29	34	30	39	25
(Heat/acid) 1X	1.11	18	17	23	13	15	25
(Heat/acid) 2X	0.71	12	15	12	10	6	12
(Heat/acid) 3X	0.75	12	12	12	7	6	10

[a] High-temperature desorption in relative values.

[b] Maximum value in this nonacid extracted sample due to the presence of a broad amorphous Al band.

the product selectivity is affected by the changes in morphology following acid extraction. All sequentially treated samples produce roughly equivalent structures with gradual increases in mesoporosity and pore size, but with constant maximum micropore volume.

SUMMARY

Figure 10 and Table 9 show the agreement among the four analytical techniques and the extent of dealumination for each mordenite sample. Structural aluminum (^{27}Al and ^{29}Si NMR), surface aluminum via XPS, strong acidity (NH$_3$ TPD), and the a_0

FIG. 10. Determination of relative Al content by various analytical techniques.

cell dimension (XRD) all follow the relative elemental aluminum concentration. The only exception to this is the XPS and TPD data for the heat-treated sample. XPS showed no change since the expelled aluminum did not migrate to the surface and TPD showed a loss of all the strong acidity. XRD, ^{29}Si, and ^{27}Al NMR remain effective techniques for determination of the extent of thermal dealumination since these methods are specific for framework aluminum. The data from the various techniques are complimentary with no technique providing complete information for all samples. However, the data from these diverse techniques give the following cohesive picture of what occurs with various sample treatments. High-temperature NH$_3$ TPD shows that strong acidity is nearly completely destroyed or at least made inaccessible by the amorphous aluminum expelled during heat treatment. Subsequent treatment with HCl removes this noncrystalline material providing access to the remaining strong acid sites. In contrast, the use of bulky TBA indicates that there are few accessible strong acid sites in fresh mordenite. Following acid dealumination, the number of strong acid sites accessible to TBA actually increases. As dealumination proceeds, a progressively smaller fraction of the remaining aluminum is strongly acidic.
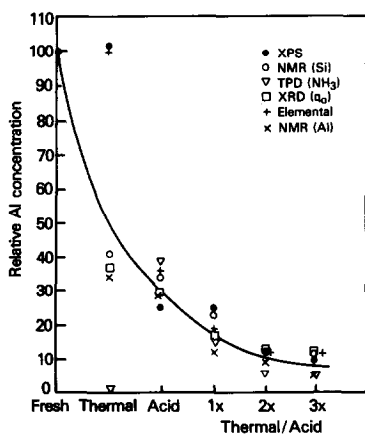
Although heat dealumination removes

approximately 70% of the structural aluminum as shown by NMR, XPS studies of the dealuminated mordenite showed the surface composition to be unchanged indicating that the amorphous aluminum formed during dry thermal treatments does not migrate. Subsequent steaming of the heat dealuminated mordenite at 500°C resulted in additional dealumination as detected by ^{27}Al NMR. Also, XPS detected a surface enrichment at the zeolite surface. It is likely that the nonstructural aluminum from thermal dealumination is immobile because aluminum migration to the crystallite surface is observed only after steaming.

Nitrogen adsorption shows that 60% of the micropore volume is blocked or filled with nonframework materials in fresh, commercial mordenite. The noncrystalline silica–aluminum in or covering the micropores is removed by acid. Changes in this micropore volume are reflected in the catalysts' selectivities for conversion of methanol to hydrocarbons. Nonstructural material present in the micropores restricts the production of bulky molecules, such as isobutane, and favors the formation of propane and propylene. Changes in morphology, however, do not explain differences in aging characteristics of the dealuminated mordenites. Long life for conversion of methanol to hydrocarbons with highly dealuminated mordenite cannot be explained on the basis of shape selectivity (29–31).

REFERENCES

1. Belenkaya, I. M., Dubinin, M. M., and Krishtofori, I. I., *ISV. Akad. Nauk. SSR Ser. Khim.*, 2164 (1967).
2. Klinowski, J., Thomas, J. M., Anderson, M. W., Fyfe, C. A., and Gobbi, G. C., *Zeolites* **3**, 5 (1983).
3. Eberly, P. E., and Kimberlin, C. N., *Ind. Eng. Chem. Prod. Res. Dev.* **9**, 335 (1970).
4. Chen, N. Y., and Smith, F. A., *Inorg. Chem.* **15**, 295 (1976).
5. Scherzer, J., *ACS Symp. Ser.* **248**, 157 (1984).
6. Topohieva, K. V., Romanovsky, B. V., Piguzova, L. I., Thoang, Ho Si, and Bizreh, Y. W. "Proceedings, 4th International Congress on Catalysis, Moscow, 1968" (B. A. Kazansky, Ed.). Adler, New York, 1968.
7. Weller, S. W., and Brauer, J. M., "AIChE 62nd Annual Meeting, Washington, DC, Nov. 16–20, 1969."
8. Kranich, W. L., Ma, Y. Y., Sand, L. B., Weiss, A. H., and Zwiebel, I., *Adv. Chem. Ser.* **101**, 502 (1970).
9. Zatorski, W., and S. Krzyzanowski, *Acta Phys. Chem.* **24**, 347 (1978).
10. Dejaifve, P., Auroux, A., Gravelle, P. C., and Vedrinl, J. C., *J. Catal.* **70**, 123 (1987).
11. Itoh, H., Hattori, T., and Murahami, Y., *Appl. Catal.* **2**, 19 (1982).
12. Cormerais, F. X., Perot, G., and Guisnet, M., *Zeolites* **1**, 141 (1981).
13. Fleisch, T. H., Ray, G. J., Meyers, B. L., and Marshall, C. L., *J. Catal.* **99**, 117 (1986).
14. Meyers, B. L., Fleisch, T. H., and Marshall, C. L., *Appl. Surf. Sci.* **26**(4), 503 (1986).
15. Mieville, R. L., and Meyers, B. L., *J. Catal.* **75**, (1982).
16. Brunauer, S., Emmett, P. H., and Teller, E., *J. Amer. Chem. Soc.* **60**, 309 (1938).
17. Barrett, E. P., Joyner, L. G., and Halenda, P. P., *J. Amer. Chem. Soc.* **73**, 373 (1951).
18. deBoer, J. H., Lippens, B. C., Linsen, B. G., and Osinga, Th. V., *J. Colloid Interface Sci.* **21**, 405 (1966).
19. Mortier, W. J., Pluth, J. J., and Smith, J. V., *Mater. Res. Bull.* **10**, 1319 (1975).
20. Mortier, W. J., Pluth, J. J., and Smith, J. V., *Mater. Res. Bull.* **11**, 15 (1976).
21. Hayes, G. R., van Erp, W. A., Alma, N. C. M., Couperus, P. A., Husi, R., and Wilson, A. E., *Zeolites* **4**, 377 (1984).
22. Debra, G., Nagy, J. B., Gabelica, Z., Bodart, P., and Jacobs, P. A., *Chem. Lett.*, 199 (1983).
23. Bodart, P., Nagy, J. B., Debras, G., Gabelica, Z., and Jacobs, P. A., *J. Phys. Chem.* **90**, 5183 (1986).
24. Englehardt, U., Lohse, U., Lippmaa, E., Tarmak, M., and Magi, M., *Z. Anorg. Allg. Chem.* **482**, 49 (1981).
25. Klinowski, J., Ramdas, S., Thomas, J. M., Fyfe, C. A., and Hartman, J. S., *J. Chem. Soc. Faraday Trans. 2* **78**, 1025 (1982).
26. Frnzke, D., Freude, D., Frohlich, T., and Haase, J., *Chem. Phys. Lett.* **111**, 171 (1984).
27. Schmidt, V. H., "Proceedings of the Ampere International Summer School II, Basko Polje, Yugoslavia, 1982."
28. Olsson, R. W., and Rollmann, L. D., *Inorg. Chem.* **16**(3), 650 (1977).
29. Rollmann, L. D., *J. Catal.* **47**, 113 (1977).
30. Walsh, D. E., and Rollmann, L. D., *J. Catal.* **49**, 369 (1977).
31. Rollmann, L. D., and Walsh, D. E., *J. Catal.* **56**, 139 (1979).